ACS OMEGA

Article

Cite This: ACS Omega 2018, 3, 15246−15255

http://pubs.acs.org/journal/acsodf

Influence of Hydration on the Structure of Reline Deep Eutectic Solvent: A Molecular Dynamics Study

Pratibha Kumari, Shobhna, Supreet Kaur, and Hemant K. Kashyap*

Department of Chemistry, Indian Institute of Technology Delhi, Hauz Khas, New Delhi 110016, India

Supporting Information

ABSTRACT: In this article, we have performed an all-atom molecular dynamics simulation study to investigate the influence of water on the molecular level arrangement of reline deep eutectic solvent for different hydration levels ranging from 3.4 to 58.1 wt % of water and complemented the observations of recently measured neutron scattering experimental data. This study is particularly important because water is being introduced as a second hydrogen bond donor/acceptor in reline, wherein the structure is primarily governed by hydrogen bonding and electrostatic interactions. We have analyzed the simulated X-ray scattering structure functions, their partial components, and hydrogen bonding interactions to understand the effects of water on various intermolecular interactions in reline−water mixtures. It is observed that at lower hydration level, reline structure is qualitatively retained. At higher hydration level, most water molecules preferentially solvate chloride anions and ammonium group of choline cations mostly impacting choline−choline, choline−chloride, and chloride−chloride interactions. The present study reveals that at and above 41 wt % of water, the molecular arrangement of reline drastically changes and set to transition from reline to an aqueous solution of reline components with further increase in the hydration level. Hydrogen bond analysis reveals the presence of strong chloride−water H-bonding interaction, which gradually replaces choline−chloride and urea−chloride hydrogen bondings as the hydration level in the mixture increases.

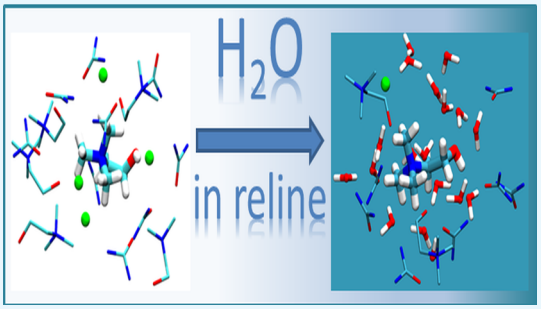

INTRODUCTION

Deep eutectic solvents (DESs) are neoteric solvents that have recently found more attention as alternative solvents owing to their low toxicity, environment benign nature, and easy preparation protocol.[1−3] Most DESs are obtained by the combination of a salt and one or more hydrogen bond donor (HBD) species such as urea, malonic acid, ethylene glycol, and amides in a specific ratio such that the finally obtained compound has a much lower melting point than its constituting components.[4−7] DESs comprised of electrolytes and amides as HBD species have also been explored recently.[8,9] The microscopic structural arrangement and properties of DESs can be tuned by selection of mixing ratio and their constituting molecular chemical moieties. This additional degree of freedom to design DESs with desired properties is encouraging to use DESs in various fields such as inorganic and organic synthesis, separation, electrochemistry, extraction, nanomaterials science, and biotransformations.[10−21] DESs are also termed as ionic liquid (IL) analogues as both share many peculiar properties. In the past, a number of studies have been performed to investigate structural morphology of pure ILs and IL + cosolvents that provide guidance to use these solvents judiciously.[22−29] However, such studies are lagging behind in case of DESs. Reline is an eutectic mixture of choline chloride and urea in a 1:2 molar ratio and is obtained from cheap, naturally occurring, and readily available starting materials.[30] It is a biodegradable, nontoxic, and economically viable solvent.[4,30] It has been used in a number of applications such as biodiesel synthesis, surface coating, electrodeposition, separation, enzymatic reactions, and carbon dioxide sequestration.[2,16,17,31−35] Because of its ability to donate and accept electrons, reline attains a high selective solubility for metal−metal oxides and is used in various metallurgical process.[36,37] It is also used as a solvent in post-etch residue removal.[38] Moreover, reline is nonreactive with water and has an acceptable toxicity profile that enables it to use as a solvent for poorly water soluble drugs.[39] It is widely accepted that the driving force for the formation of reline is the charge delocalization because of hydrogen bonding (H-bonding) interaction between the chloride anion and urea. Recent studies based on the neutron diffraction (ND) experiment, empirical potential structure refinement (EPSR) and molecular dynamics (MD) simulation provide a significant insight into the molecular level arrangement of different constituting species of reline.[7,40,41] These studies support the proposition that each chloride anion (Cl^-) is stabilized by two urea molecules via H-bonding interaction and to better accommodate urea within the H-bonded complex, most Cl^- anions are positioned near the hydroxyl group of choline cations (Ch^+).

Received: September 20, 2018
Accepted: October 23, 2018
Published: November 12, 2018

DOI: 10.1021/acsomega.8b02447
ACS Omega 2018, 3, 15246−15255

In reline, both urea and choline chloride are hygroscopic in nature, and it has been observed via experimental and simulation studies that the presence of little amount of water as a second HBD species not only changes the macroscopic properties such as density, ionic conductivity, and viscosity but also disturbs the favorable molecular arrangement in DES compounds, which eventually curbs their use in various applications.[42] Further, the preferred molecular organization of pure DESs provides an ideal environment for selective catalysis or nanoparticle synthesis. The presence of water, however, could limit the use of it in such applications. Therefore, quantification of water content in DESs is necessary before employing it for any physicochemical characterization and for any application.

Recently, few experimental[42−45] and simulation[42,46] studies have been performed on reline−water mixtures to understand the effect of water on the physicochemical properties and molecular arrangement of reline to a certain extent. Shah and Mjalli have performed the experimental and MD simulation study on aqueous reline and showed that thermophysical properties such as density, viscosity, melting point, and refractive index vary gradually with addition of water. Their H-bond analysis revealed that at low water content, urea−urea and cation−urea interactions increase but at higher water concentration (beyond >25 wt %), the constituting species of reline are individually hydrated and show high diffusivity.[42]

By employing the neutron scattering experiment, Edler and co-workers[44] have shown that the reline microscopic structure retains up to 42 wt % of water content because of solvophobic sequestration of water into the nanostructure domains around choline cations. However, at 51 wt % of water content, the DES structure is disturbed and eventually leads to transition from reline to an aqueous solution of reline components.[44] By using pulsed field gradient NMR diffusion measurements, D'Agostino and co-workers[43] observed that with addition of water, Ch^+ cations diffuse in the Stokesian manner and lead to exchange of the hydroxyl proton on Ch^+. Note that such exchange of proton is technically not possible to observe in the present MD simulation study. Their study also indicates that regardless of hydrophilic nature of the choline chloride salt and HBD species, their aqueous solution forms inhomogeneous complex mixtures at the microscopic level. By using Brillouin spectroscopy and ^{1}H NMR, Posada et al. also confirmed these inhomogeneities despite their fully miscible appearance at the macroscopic level.[45] However, these two studies differ in the hydration level at which this phase segregation occurs. Pandey and Pandey[47] spectroscopic study on reline−water proposed the interstitial accommodation of water within the H-bonded network of reline components. Recently, Siepmann and co-workers[46] carried out first principle MD simulations of pure reline and its equimolar mixture with water and showed that in hydrated DES, water competes for Cl^- anions and disrupts H-bonding interaction between urea and Cl^-. The hydrogen atoms (H-atom) of urea have equal probability to H-bond with Cl^- anions and with the oxygen atom of urea and water.[46]

Recent studies performed on understanding the structure of pure reline pointed out the importance of H-bonding interaction of Cl^- with the amide group of urea and hydroxyl group of Ch^+ cations in determining the molecular level arrangement in reline.[7,40,41] The MD investigation performed on aqueous reline majorly focused on the influence of water on H-bonding behavior of urea−Cl^- interaction and how these two species interact with water.[42,46] Because Ch^+−Cl^- and Ch^+−Ch^+ interaction are also substantially affected by the presence of water,[44] in order to get further insights, herein, we have explored all possible H-bonding interactions for a wide range of hydration levels. Another peculiar feature which is already mentioned in the previous study by our group[40] on pure reline is the presence of long-range ordering which is observed only through partial X-ray scattering structure functions. This low q (below q = 1 Å^{-1}) feature is basically because of the presence of strong positive correlation between co-ionic species and negative correlation between counter-ionic species and cation−urea. However, because of cancellation effects, no low q peak is observed in the total X-ray scattering structure function of reline. Hence, it is crucial to understand the effect of hydration on these long-range correlations. In this spirit, herein, we present an atomistic MD study of reline−water mixtures containing 3.4, 6.5, 12.2, 21.7, 41.0, and 58.1 wt % of water to shed more light on how the inverse and real-space correlations between different species of reline are influenced at various hydration levels. We have analyzed simulated X-ray scattering structure functions and their partial components, hydrogen bonding interactions, radial and three-dimensional spatial distribution functions (SDFs) for reline−water mixtures and compared with that for pure reline.

COMPUTATIONAL DETAILS

The MD simulations were carried out using GPU version of the GROMACS-5.1.1 (single precision) package.[48,49] Please refer to Figure 1 for chemical structures of reline components.

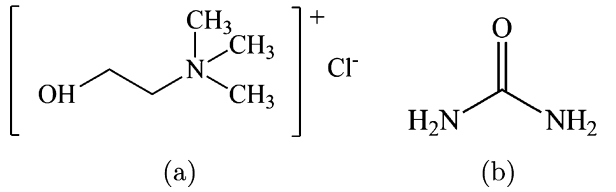

Figure 1. Chemical structure of (a) choline chloride and (b) urea.

All species constituting reline (Ch^+, Cl^-, and urea) were modeled using CHARMM 36 force field[21,50] parameters as reported in the recent MD simulation study from our group.[40] The validity of the force-field used for pure reline was checked against ND experimental data[7] and experimental bulk density.[51] The simulated neutron scattering data including low q region are in good agreement with experimental neutron scattering data. In order to further verify the robustness of the force-field used here, we have carried out another MD simulation by utilizing the non-bonded parameter Lennard-Jones terms and partial charges suggested by ND/EPSR modeling[7] and the bonded parameter from optimized potential for liquid simulations (OPLS) force field and computed neutron scattering $S(q)$ and compared against its experimental counterpart. A comparative plot showing the simulated and experimental[7] $S(q)$s for pure reline are shown in Figure S1 of the Supporting Information. The figure clearly shows that CHARMM 36 is not only in good agreement with the experiment but also it is as good as OPLS force field. Additionally, in Table S1 of the Supporting Information, the average coordination number and peak positions of the first solvation peak of the center-of-mass radial distribution functions (RDFs) between different constituent species of reline obtained through CHARMM 36 force field is compared

DOI: 10.1021/acsomega.8b02447
ACS Omega 2018, 3, 15246−15255

with the Hammond et al. ND/EPSR study.[7] A fair agreement between the average coordination number and maximum and minimum of the first peak (r_{max} and r_{min}) compared to ND/EPSR is observed. Although CHARMM 36 has sharper peaks with larger peak intensity compared to the ND/EPSR study, the average coordination numbers are found within statistical uncertainties. The SPC/E water model[52] was used for water. The initial cubic simulation boxes consisted of 1000 ion pairs of choline chloride (Ch^+-Cl^-), 2000 molecules of urea, and desired number of water molecules were generated using the PACKMOL[53] package. A summary of the reline−water systems simulated in the present study is provided in Table 1 and chemical structures of Ch^+ cation and urea with partial

Table 1. Summary of the Reline−Water Mixtures Studied in the Present Work

			no. of molecules		
system	reline (wt %)	water (wt %)	Ch^+-Cl^-	urea	water
rel−0.5w	96.6	3.4	1000	2000	500
rel−1w	93.5	6.5	1000	2000	1000
rel−2w	87.8	12.2	1000	2000	2000
rel−4w	78.3	21.7	1000	2000	4000
rel−10w	59.0	41.0	1000	2000	10 000
rel−20w	41.9	58.1	1000	2000	20 000

atomic charges are provided in Figure S2 of the Supporting Information. A cubic box containing 1000 molecules of water was also generated utilizing PACKMOL for pure water simulation. Periodic boundary conditions and minimum image convention were applied in all three directions of the simulation box. To evaluate electrostatic interactions particle mesh Ewald (PME)[54,55] summation method with an interpolation order of 6 and a Fourier grid spacing of 0.8 Å were used. For short range interactions, the cut-off radius was set to 12 Å with a switching function used from 10 to 12 Å. The equations of motion were integrated using the leap-frog algorithm with 1 fs time step. All hydrated reline systems were equilibrated in *NPT* ensemble for 60−70 ns at 303 K temperature and 1 bar pressure. The temperature and pressure of systems were maintained using Nosé−Hoover thermostat[56−58] and Parrinello−Rahman barostat,[59] respectively. To compute properties of the equilibrated systems, 10 ns of production run was carried out and trajectories were saved at every 100 fs.

In order to compare the properties of reline−water mixtures with pure reline, we have adapted the production run trajectory from the previously simulated pure reline from our group[40] and computed desired properties.

The total X-ray scattering static structure function, $S(q)$, was computed using the methodology provided in the literature[24] as

$$S(q) = \frac{\rho_o \sum_{i=1}^{n}\sum_{j=1}^{n} x_i x_j f_i(q) f_j(q) \int_0^{L/2} 4\pi r^2 [g_{ij}(r) - 1] \frac{\sin qr}{qr} \omega(r) dr}{[\sum_{i=1}^{n} x_i f_i(q)]\left[\sum_{j=1}^{n} x_j f_j(q)\right]} \quad (1)$$

Here, $g_{ij}(r)$ refers to partial RDFs, for the atoms of type i and j involving both intra- and intermolecular pairs. x_i and x_j denote the mole fraction of atom types i and j, respectively. $f_i(q)$ and $f_j(q)$ are the X-ray atomic form factors.[60] L is the average box length, and ρ_o is total number density. Lorch window function, $\omega(r)$, could be used to reduce the effect of the finite truncation error on the integral; $\omega(r) = \sin(2\pi r/L)/(2\pi r/L)$.

Partial components of the total X-ray structure function were computed for reline−water mixtures to understand the origin of different peaks observed in the total $S(q)$s. We have used the following scheme for splitting the total $S(q)$ into its species-wise partial components[26,40]

$$S(q) = S^{Ch^+-Ch^+}(q) + S^{Cl^--Cl^-}(q) + S^{urea-urea}(q) + S^{water-water}(q) + 2S^{Ch^+-Cl^-}(q) + 2S^{Ch^+-urea} + 2S^{Ch^+-water} + 2S^{Cl^--urea} + 2S^{Cl^--water} + 2S^{urea-water} \quad (2)$$

Three-dimensional SDFs were calculated using TRAVIS[61] and rendered by the visual MD (VMD) package.[62] To define a hydrogen bond, a distance cut-off of 3.5 Å between donor and acceptor atoms and hydrogen−donor−acceptor angle less than 30° were taken as the geometrical criteria.

RESULTS AND DISCUSSION

Comparison of Simulated Density Against Experimental Data. In order to validate the force field used for the aqueous reline systems simulated here, we have computed the bulk densities for the whole range of composition studied and compared against the experimental values. Figure 2 shows a

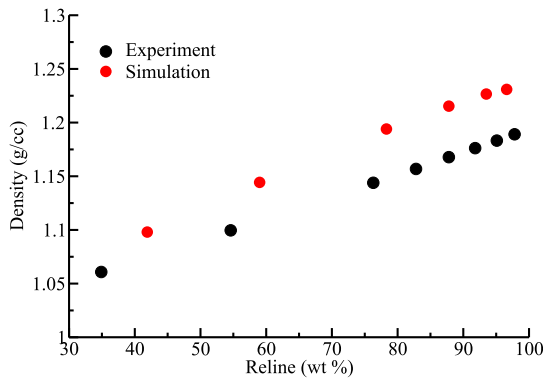

Figure 2. Comparison of simulated and experimental densities as a function of reline wt % for the reline-water mixture.

comparison of simulated density with the experimental data[51] for the reline−water mixtures as a function of the reline wt % (refer to Table S2 for the tabulated data). The agreement between the simulation and experiment is found to be fairly good over the entire composition range investigated here.

X-ray Scattering Static Structure Functions and Their Partial Components. Figure 3 shows the X-ray scattering total structure functions, $S(q)$s, for water, pure reline, and reline−water mixtures computed using eq 1. We can observe that the pure reline system shows a principal peak at around q = 1.6 $Å^{-1}$ which corresponds to a real-space distance of 3.9 Å, whereas pure water shows two peaks centered around q = 2.1 and q = 2.8 $Å^{-1}$ resembling two real-space distances of about 3.0 and 2.2 Å. Figure 3 shows that the most prominent peak (q = 1.6 $Å^{-1}$) in the $S(q)$ of pure reline shifts toward higher q values or shorter characteristic real-space length scales with a gradual decrease in its intensity upon addition of water in reline. Further, reaching on to a system containing the highest

DOI: 10.1021/acsomega.8b02447
ACS Omega 2018, 3, 15246−15255

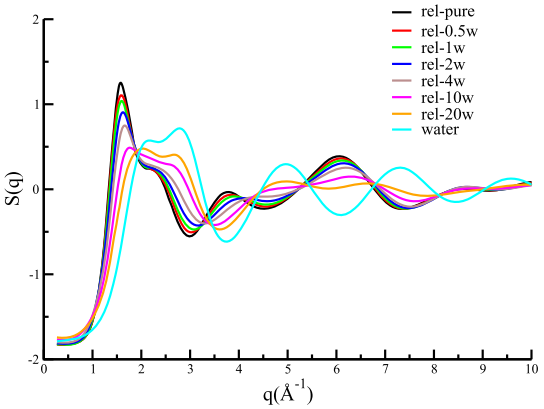

Figure 3. Simulated X-ray scattering total structure functions, $S(q)$s, for reline–water mixtures at different hydration levels. The $S(q)$s for pure reline and water are also shown for comparison. Pure reline data were taken from the recently published article from our group.[40]

hydration level in the present study, this peak is almost diminished. Moreover, a new peak at a larger q value corresponding to that of pure water emerges along with continuously shifting and fading of the reline characteristic peak with addition of water in the DES. Similar to that of the pure water system, the rel–20w (containing 58.1 wt % water) system shows two peaks at around q = 2 and 2.7 Å^{-1} indicating a transition of intermolecular arrangement from reline to that of water. The shift of the reline characteristic peak to shorter length scales (higher q values) with increase in water content shows a contraction in the major intermolecular interaction distance from 3.9 to 3.1 Å. These observations are in corroboration with recent ND experiments performed for a range of reline–water (D_2O) mixtures by Edler and co-workers.[44] The experimental ND data also show merging of the characteristic peak of pure deuterated reline with the D_2O peak at higher hydration level.

The significance of partitioning of total X-ray scattering structure function into its partial components for neat reline has been previously reported by our group.[40] As anticipated

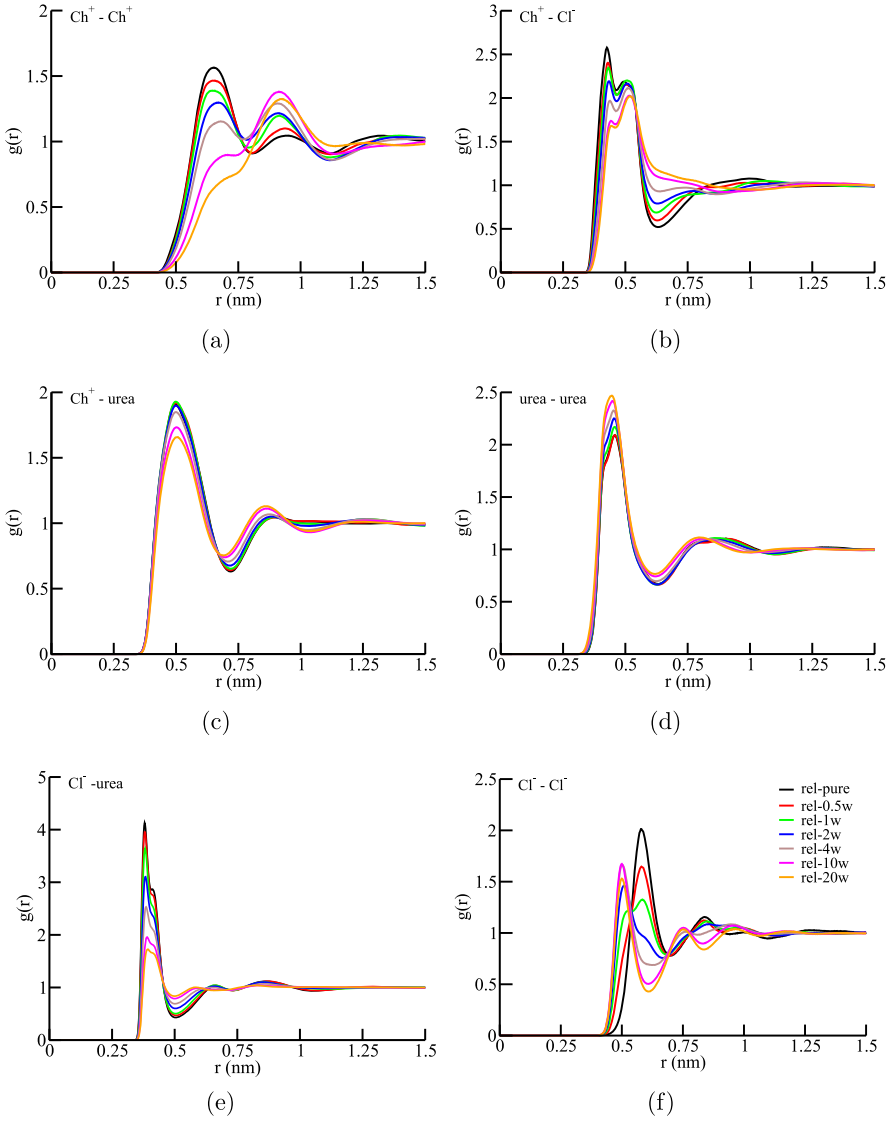

Figure 4. Intermolecular center-of-mass RDFs, $g(r)$, for (a) Ch^+–Ch^+, (b) Ch^+–Cl^-, (c) Ch^+–urea, (d) urea–urea, (e) Cl^-–urea, and (f) Cl^-–Cl^- in reline–water mixtures. The RDF data for pure reline were taken from Kaur et al.[40]

DOI: 10.1021/acsomega.8b02447
ACS Omega 2018, 3, 15246–15255

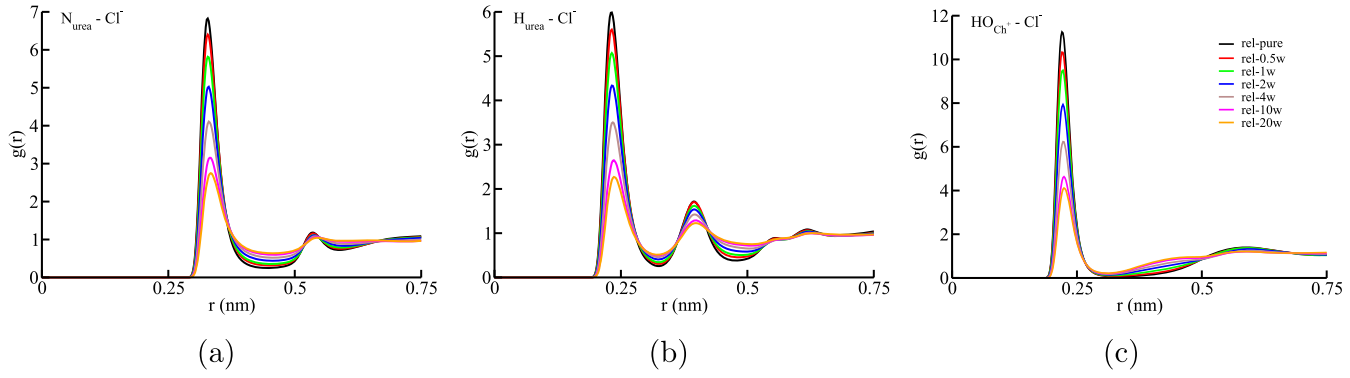

Figure 5. Atomic RDFs, $g(r)$, for (a) N_{urea}−Cl^-, (b) H_{urea}−Cl^-, and (c) HO_{Ch^+}−Cl^- pairs in reline−water mixtures. Here, N_{urea} and H_{urea} denote nitrogen and hydrogen atoms of amide groups of urea, whereas HO_{Ch^+} represents hydroxyl hydrogen of the Ch^+ cation. RDFs for pure reline are also shown for comparison.[40]

from the partial structure functions, the major contribution to the principal peak is due to positive urea−urea and Ch^+−urea correlations along with little participation of Ch^+−Cl^- correlations. However, through the partitioning of the total X-ray $S(q)$s for all reline−water mixtures, we observe that the addition of water causes depreciation in these correlations leading to diminished intensity of the principal peak (refer to Figure S3).

Another important feature observed through the partial components of total $S(q)$ is the long-range ordering, that is peaks and antipeaks displayed by partial $S(q)$s in the low q region ($0.8 < q/Å^{-1} < 1.0$), which is absent in the total X-ray $S(q)$.[40] We find that the addition of water decreases the amplitudes of peaks for Ch^+−Ch^+ and urea−urea correlations and antipeaks for Ch^+−urea and Ch^+−Cl^- correlations in the low q region along with their shifts toward larger length scales as shown in Figure S3. This demonstrates the disruption of long-range ordering in the mixture with the rise of water content. In Figure S4, the presence of long-range correlations in the lower q region corresponding to Ch^+−water, urea−water, Cl^-−water, and water−water can also be seen. The antipeak for cation−water gets pronounced with increasing water wt % upto rel−10w along with a slight increase in intensity of the peak for water−water at the same length scale in the lower q region. In summary, hydration not only affects the close contact correlations (anticipated from the principal peak) but also alters the arrangement of reline−water components at longer distances.

Intermolecular RDFs. In order to understand the influence of water on the intermolecular interactions of reline components, we have analyzed center-of-mass RDFs shown in Figure 4a−f. From Figure 4a, one can observe that for Ch^+−Ch^+ correlation, the position of the first solvation peak shifts toward longer length scale along with a gradual decrease in its intensity with increasing water concentration. This indicates that Ch^+−Ch^+ correlation becomes weaker, and the nearest neighbor distance between Ch^+−Ch^+ increases with increase in water concentration. Furthermore, for the rel−20w system, the peak corresponding to the first solvation shell in the neat reline system almost disappears implying that with increase in water concentration, the water molecules come in closer proximity of Ch^+ than other Ch^+ ions. These observations are further explained through the analysis of H-bonding interactions and SDFs discussed in the later sections.

Figure 4b,e manifest that for the pure reline system, urea−Cl^- correlation is more prominent than Ch^+−Cl^- correlation, indicating the significance of urea−Cl^- correlation for rendering DES nature of reline which is also consistent with the previous studies on pure reline.[7,40,46] The intensities of the nearest neighbor peaks of Ch^+−Cl^- and urea−Cl^- correlations decrease with the addition of water, however, the positions of the peaks remain unaffected for the entire concentration range of reline−water mixtures investigated. This points out that at a particular separation, the probability of finding these pairs with respect to the bulk value decreases as the water concentration increases. On the other hand, urea−urea correlation becomes stronger, and the position of the nearest neighbor peak of urea−urea RDF slightly shifts toward shorter length scale than that in pure reline on the addition of water as evident from Figure 4d.

Figure 4c indicates that Ch^+−urea correlation depends on the concentration of water present in reline−water systems. At lower water concentration (up to rel−2w system), there is a slight increase in Ch^+−urea correlation, whereas at a higher hydration level, Ch^+−urea correlation decreases. This observation is further explained through atomic RDFs discussed later on. The intensity of the nearest neighbor peak for Cl^-−Cl^- correlation (Figure 4f) decreases with addition of water up to the rel−1w system after which a newly emerged solvation peak at a shorter distance is observed. This suggest that Cl^- ions come closer in the presence of water as compared to neat reline. In addition, refer to Figure S5a and Table S3 of the Supporting Information for the corresponding coordination numbers at different compositions of the mixture. Center-of-mass RDFs and composition-dependent coordination numbers for Ch^+−water, urea−water, Cl^-−water, and water−water correlations are shown in Figures S6, S5b, and Table S4. Figure S5b and Table S4 clearly show that coordination numbers for reline components−water increases with increasing the hydration level in the mixture.

Hydrogen Bonding. In the past, it has been shown that in pure reline, the specific H-bonding interactions of Cl^- anions with hydroxyl hydrogen of Ch^+ cations (HO_{Ch^+}) and urea hydrogen atoms (H_{urea}) play a central role to cater the eutectic nature of reline.[40] In order to understand how the presence of water affects these H-bonding interactions, we have computed atomic RDFs for N_{urea}−Cl^-, H_{urea}−Cl^-, and HO_{Ch^+}−Cl^- pairs as shown in Figure 5a−c. It is apparent from Figure 5 that the Cl^- anion has substantial H-bonding interactions with hydroxyl hydrogen of Ch^+ and amide groups of urea in neat reline. With addition of water in reline, the intensities of the first solvation peaks of these atomic RDFs continuously

DOI: 10.1021/acsomega.8b02447
ACS Omega 2018, 3, 15246−15255

decrease, suggesting a decrease in the probability of finding the nearest neighbor. Hence, the H-bonding interactions of the Ch^+ hydroxyl group and amide groups of urea with the Cl^- anion get weaker in the presence of water. In addition, we have also studied the effect of hydration on H-bonding interaction between Ch^+ cations and urea through HO_{Ch^+}–O_{urea} RDF shown in Figure 6. The H-bonding interaction between urea

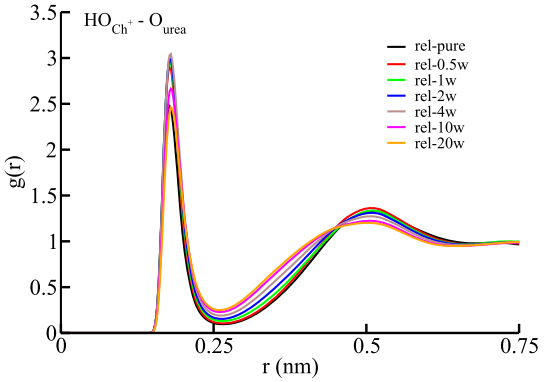

Figure 6. Atomic RDFs, $g(r)$, for HO_{Ch^+}–O_{urea} pair in reline–water systems. Here, HO_{Ch^+} and O_{urea} represents hydroxyl hydrogen of the Ch^+ cation and oxygen atom of urea, respectively. RDF for pure reline is also shown for comparison.

oxygen (O_{urea}) and Ch^+ hydroxyl hydrogen (HO_{Ch^+}) depends on the amount of water in the reline–water mixture. At lower wt % of water, there is slight increase in the H-bonding interaction between HO_{Ch^+}–O_{urea} as compared to neat reline. However, further increase in water concentration reduces this H-bonding interaction. This observation is in accordance with center-of-mass Ch^+–urea correlation as discussed in Figure 4c.

We have also investigated the various H-bonding interactions between water and reline constituting species through atomic RDFs depicted in Figure 7a–d. Among all H-bonding interactions present between water and various reline species, Cl^- anions show the most intense H-bonding tendency with water (see Figure 7a), which implies to substantial hydration of the Cl^- anion as compared to other species. This observation is also confirmed through the presence of the highest number of H-bonds between Cl^- anions and water shown in Figure S7 of the Supporting Information. In addition to this, from Figures 5c and 7b,c we observe that there is an enhance tendency of water molecules to get closer to hydroxyl group of the cation with increasing water content as depicted from peak position values (refer to Tables S5 and S6).

The variation in the number of H-bonds with time for all possible H-bonding interactions in neat reline and reline–water mixtures is shown in Figure S7 of the Supporting Information. The corresponding average number of H-bonds is also provided in Table S7 of the Supporting Information. The numbers of H-bonds between hydroxyl group of Ch^+ ($OHCh^+$)–Cl^- and amide groups of urea (NH_{urea})–Cl^- decrease and Cl^-–water increases monotonically with increasing hydration level. This clearly demonstrates that when water is introduced in pure reline, it preferentially starts solvating Cl^- anions. It can also be observed that the average number of H-bonds increases for Ch^+–water pair as compared to Ch^+–Cl^- pair which supports the notion of increasing tendency of water molecules to come closer to Ch^+ cations. The H-bond analysis of $OHCh^+$–O_{urea} shows non-monotonic behavior with the addition of water as mentioned previously.

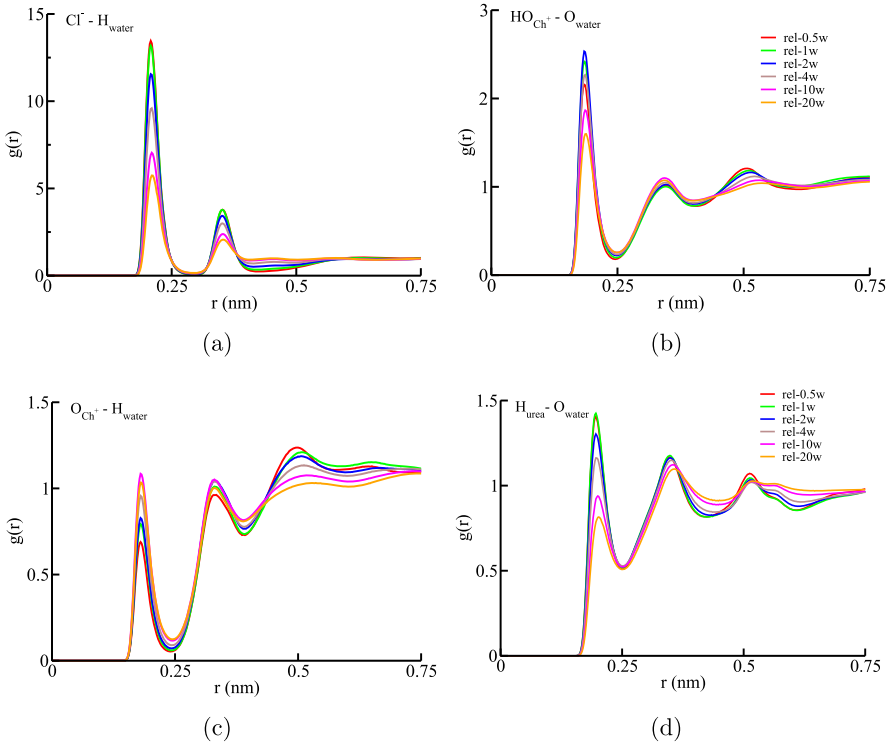

Figure 7. Atomic RDFs, $g(r)$, for (a) Cl^-–H_{water}, (b) HO_{Ch^+}–O_{water}, (c) O_{Ch^+}–H_{water}, and (d) H_{urea}–O_{water} pairs showing H-bonding interactions in reline–water mixtures. Here, H_{water} and O_{water} represent hydrogen and oxygen atoms of water, respectively. O_{Ch^+} denotes hydroxyl oxygen atom of the Ch^+ cation. Other denotations are same as mentioned in Figure 5.

DOI: 10.1021/acsomega.8b02447
ACS Omega 2018, 3, 15246–15255

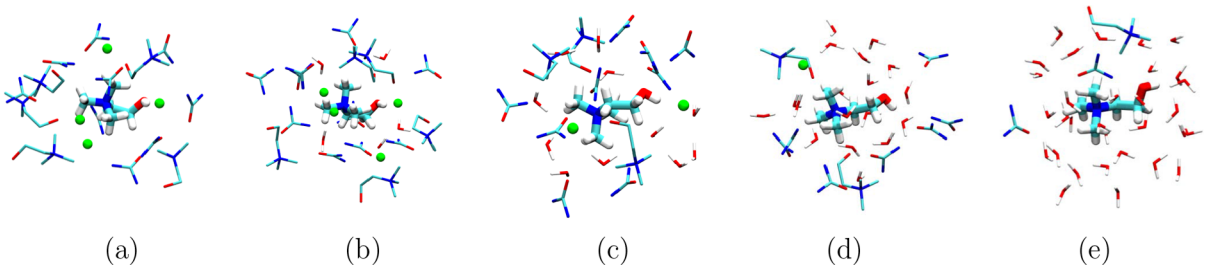

Figure 8. Molecular representation of the arrangement of Ch^+ cations, Cl^- anions, urea, and water molecules around a distance of 4 Å from the central Ch^+ cation molecule for (a) pure reline, (b) rel−0.5w, (c) rel−4w, (d) rel−10w, and (e) rel−20w systems containing 0, 3.4, 21.7, 41, and 58.1 wt % water, respectively. In the snapshots, nitrogen, oxygen, carbon, and hydrogen atoms of Ch^+ cations, urea, and water are shown as blue, red, cyan, and white stick, respectively. Cl^- anions are rendered as green spheres. Decrease in the numbers of Cl^- anions and other reline constituting species along with increase in the number of water molecules around the cation is clearly visible as the hydration level in the mixture increases.

At lower hydration level, the $OHCh^+-O_{urea}$ H-bonding interactions tend to increase with increase in water concentration, but as we move beyond the rel−2w system, the H-bonding propensity diminishes. This behavior corresponds to enhanced tendency of water molecules to be in vicinity of cations and urea. In the past, Shah and Mjalli[42] also observed preferential hydration of the Cl^- anion as compared to cation or urea molecule in aqueous reline. Another MD simulation study performed by Gao and co-workers[63] on reline−water mixtures also reported that hydration strength of the Cl^- anion is stronger than Ch^+ cation over all water fraction investigated.

The analysis of center-of-mass RDFs and H-bonding stipulate the subtle changes in the molecular arrangement of reline species around Ch^+ cations upon introduction of water in the pure reline system. In order to visualize this fact, in Figure 8, we have rendered the representative molecular arrangement of different reline species within a distance of 4 Å from the central Ch^+ cation for pure reline and different reline−water mixtures. In pure reline, we can see the preferred H-bonding interactions between Cl^- anions and urea molecules. Figure 8a indicates that pure reline has 4 Cl^- anions around Ch^+ cation which shows H-bonding interactions with hydroxyl hydrogen of Ch^+ cation and with amide hydrogens of urea molecules. The reline−water system containing 3.4 wt % of water still have 4 Cl^- anions around the Ch^+ cation; however, each Cl^- anion is followed by a water molecule suggesting that water first starts solvating Cl^- anions. Further increase in water content increases the number of water molecules and reduces the presence of Ch^+, Cl^-, and urea molecules around the Ch^+ cation. The rel−4w system shows 2 Cl^- anions, one Cl^- pointing toward the hydroxyl hydrogen of the Ch^+ cation indicating the existence of preferred H-bonding interaction between the Ch^+ cation and Cl^- anion. However, in case of the rel−10w system, most Cl^- anions are replaced with water molecules as evident from Figure 8d, suggesting the substitution of Ch^+-Cl^- H-bond with Ch^+−water. At the highest hydration level, we can observe the presence of a solvation shell of water molecules around Ch^+ cation as most of the reline−reline H-bonding pairs are replaced with reline−water H-bonding pairs.

Spatial Distribution Functions. SDFs showing the nearest solvation shells of Cl^- anions and Ch^+ cations around Ch^+ cation in the pure reline and reline−water mixtures containing 3.4, 21.7, and 41 wt % of water (corresponding to rel−0.5w, rel−4w, and rel−10w systems, respectively) are depicted in Figure 9a−d. Along with this, we have also shown

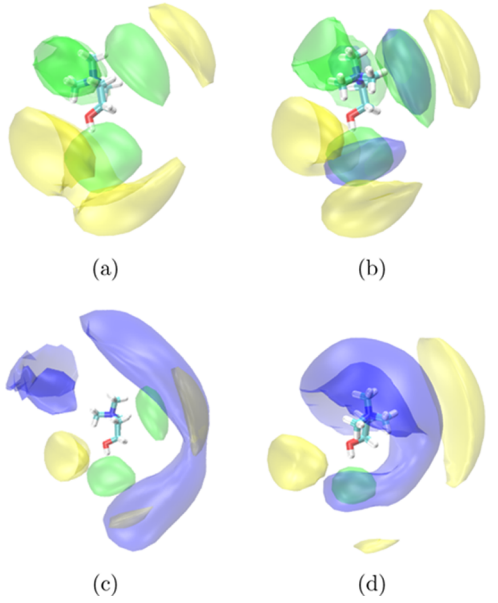

Figure 9. SDFs of Ch^+ (yellow, transparent), Cl^- (green, transparent), and water (blue, transparent) around the Ch^+ cation for (a) pure reline, (b) rel−0.5w, (c) rel−4w, and (d) rel−10w systems containing 0, 3.4, 21.7, and 41 wt % water, respectively.

the SDF of water around Ch^+ cation to get a qualitative picture of change in the arrangement of water with increasing hydration level. We observe that water and Cl^- anion compete for the Ch^+ cation as the Cl^- isodensity surface is intervened by that of water with increase in water concentration. This observation corroborates with the previously mentioned real-space correlations shown in Figure 4b.

Another significant observation is the change in isosurface density of cations around a central cation. As water is added in reline, it starts irrupting near the hydroxyl and ammonium groups of Ch^+ but at a closer distance than other Ch^+ owing to enhanced H-bonding interactions between the Ch^+ hydroxyl group and water molecules, which is also previously seen in the RDFs (see Figure 7b,c). As evident from Figure 9b−d, the density surface of water around Ch^+ increases with increase in water concentration, also indicating that water molecules gradually push Ch^+ cations apart.

SDFs showing the nearest solvation shell of Ch^+ cations and Cl^- anions around urea for pure reline and reline−water mixtures containing 3.4, 21.7, and 41 wt % of water are depicted in Figure 10a−d. The isodensity surface of water

DOI: 10.1021/acsomega.8b02447
ACS Omega 2018, 3, 15246−15255

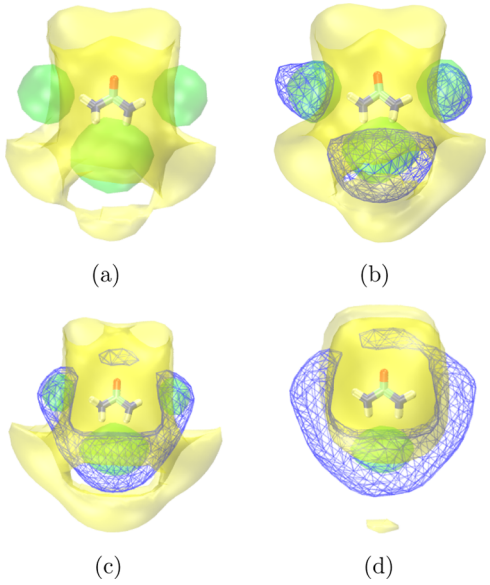

Figure 10. SDFs of Ch^+ (yellow, transparent), Cl^- (green, transparent), and water (blue, wired frame) around urea for (a) pure reline, (b) rel−0.5w, (c) rel−4w, and (d) rel−10w systems containing 0, 3.4, 21.7, and 41 wt % water, respectively.

around urea is also shown in Figure 10b−d for reline−water systems. For pure reline, Cl^- anion lobs are pointed toward amide hydrogens, whereas Ch^+ cation isodensity surface takes positions all around urea molecule as manifested in Figure 10a. When water is introduced in reline, it starts solvating Cl^- anions first and then approaches to the oxygen atom of the urea molecule at higher water concentration as evident from Figure 10b−d. Hence, it is apparent that with increase in water concentration, isodensity surface of Cl^- anions around urea starts decreasing, whereas that of water starts increasing, thus affirming the decrease in urea−Cl^- H-bonding intensity. The isodensity surface of Ch^+ cations around urea shows concentration-dependent behavior similar to what is observed in corresponding RDF described in Figure 4c.

CONCLUSIONS

We have reported an all-atom MD simulation study to provide an insight on how intermolecular and H-bonding interactions between different species of reline are affected when water is introduced in reline across a wide range of hydration levels. It was shown that the presence of water gradually reduces the various interactions between the components of reline. The examination of SDFs and RDFs revealed that when water is added in reline, it preferentially solvates Cl^- anions and ammonium and hydroxyl groups of Ch^+ cations. It was observed that at higher hydration level, Ch^+−Ch^+, Ch^+−Cl^-, and Cl^-−Cl^- interactions are most intensely affected as the water molecules systematically arrange themselves around Cl^- and choline hydroxyl group at a shorter distance than urea and Cl^- via H-bonding interaction. As also observed in the neutron scattering experiments,[44] the simulated X-ray scattering structure functions showed that below 41 wt % water level, the reline structure is qualitatively retained, indicating 41 wt % of water is the transition point above which the mixture turns into an aqueous solution of reline components. We conclude by noting that further simulation studies are required for understanding the interfacial structure of the reline−water system near electrode materials for their optimum use in advance energy storage devices.[64]

ASSOCIATED CONTENT

Supporting Information

The Supporting Information is available free of charge on the ACS Publications website at DOI: 10.1021/acsomega.8b02447.

Tables for coordination number and peak positions for pure reline system, experimental and simulated densities, coordination number and peak positions for center-of-mass and atomic RDFs for reline−water mixtures, and average H-bond number, and figures for neutron $S(q)$s, chemical structure, partial X-ray $S(q)$s, center-of-mass RDFs for different reline components−water, composition dependence of coordination numbers, and H-bond numbers (PDF)

AUTHOR INFORMATION

Corresponding Author

*E-mail: hkashyap@chemistry.iitd.ac.in. Phone: +91-(0)11-26591518. Fax: +91-(0)11-26581102.

ORCID

Hemant K. Kashyap: 0000-0001-9124-2918

Notes

The authors declare no competing financial interest.

ACKNOWLEDGMENTS

We thank Professor Karen J. Edler for providing the experimental neutron scattering data for pure reline. We sincerely thank Professor Ranjit Biswas, Professor Claudio J. Margulis, and Professor Edward W. Castner, Jr. for support and encouragement. P.K. thanks IIT Delhi and Shobhna, and S.K. thank UGC, India, for fellowships. P.K. also thanks Sraddha Agrawal for technical help. This work is financially supported by the Department of Science and Technology (DST), India, through FIST grant, and a grant awarded to H.K.K. (grant no. SB/FT/CS-124/2014).

REFERENCES

(1) Smith, E. L.; Abbott, A. P.; Ryder, K. S. Deep Eutectic Solvents (DESs) and Their Applications. *Chem. Rev.* **2014**, *114*, 11060−11082.
(2) Zhang, Q.; De Oliveira Vigier, K.; Royer, S.; Jérôme, F. Deep Eutectic Solvents: Syntheses, Properties and Applications. *Chem. Soc. Rev.* **2012**, *41*, 7108−7146.
(3) Clarke, C. J.; Tu, W.-C.; Levers, O.; Bröhl, A.; Hallett, J. P. Green and Sustainable Solvents in Chemical Processes. *Chem. Rev.* **2018**, *118*, 747−800.
(4) Abbott, A. P.; Boothby, D.; Capper, G.; Davies, D. L.; Rasheed, R. K. Deep Eutectic Solvents Formed between Choline Chloride and Carboxylic Acids: Versatile Alternatives to Ionic Liquids. *J. Am. Chem. Soc.* **2004**, *126*, 9142−9147.
(5) Kaur, S.; Gupta, A.; Kashyap, H. K. Nanoscale Spatial Heterogeneity in Deep Eutectic Solvents. *J. Phys. Chem. B* **2016**, *120*, 6712−6720.
(6) Kaur, S.; Kashyap, H. K. Unusual Temperature Dependence of Nanoscale Structural Organization in Deep Eutectic Solvents. *J. Phys. Chem. B* **2018**, *122*, 5242−5250.
(7) Hammond, O. S.; Bowron, D. T.; Edler, K. J. Liquid Structure of the Choline Chloride-Urea Deep Eutectic Solvent (Reline) from Neutron Diffraction and Atomistic Modelling. *Green Chem.* **2016**, *18*, 2736−2744.

DOI: 10.1021/acsomega.8b02447
ACS Omega 2018, 3, 15246−15255

(8) Das, S.; Mukherjee, B.; Biswas, R. Microstructures and Their Lifetimes in Acetamide/Electrolyte Deep Eutectics: Anion Dependence. *J. Chem. Sci.* **2017**, *129*, 939−951.
(9) Guchhait, B.; Das, S.; Daschakraborty, S.; Biswas, R. Interaction and Dynamics of (Alkylamide + Electrolyte) Deep Eutectics: Dependence on Alkyl Chain-length, Temperature, and Anion Identity. *J. Chem. Phys.* **2014**, *140*, 104514.
(10) Abbott, A. P.; Alhaji, A. I.; Ryder, K. S.; Horne, M.; Rodopoulos, T. Electrodeposition of Copper−Tin Alloys Using Deep Eutectic Solvents. *Trans. IMF* **2016**, *94*, 104−113.
(11) Das, S.; Mondal, A.; Balasubramanian, S. Recent Advances in Modeling Green Solvents. *Curr. Opin. Green Sustain. Chem.* **2017**, *5*, 37−43.
(12) Carriazo, D.; Serrano, M. C.; Gutiérrez, M. C.; Ferrer, M. L.; del Monte, F. Deep-Eutectic Solvents Playing Multiple Roles in the Synthesis of Polymers and Related Materials. *Chem. Soc. Rev.* **2012**, *41*, 4996−5014.
(13) Wagle, D. V.; Zhao, H.; Baker, G. A. Deep Eutectic Solvents: Sustainable Media for Nanoscale and Functional Materials. *Acc. Chem. Res.* **2014**, *47*, 2299−2308.
(14) Raghuwanshi, V. S.; Ochmann, M.; Polzer, F.; Hoell, A.; Rademann, K. Self-Assembly of Gold Nanoparticles on Deep Eutectic Solvent (DES) Surfaces. *Chem. Commun.* **2014**, *50*, 8693−8696.
(15) Abbott, A. P.; Ttaib, K. E.; Frisch, G.; Ryder, K. S.; Weston, D. The Electrodeposition of Silver Composites Using Deep Eutectic Solvents. *Phys. Chem. Chem. Phys.* **2012**, *14*, 2443−2449.
(16) Liao, Y.-S.; Chen, P.-Y.; Sun, I.-W. Electrochemical Study and Recovery of Pb Using 1:2 Choline Chloride/Urea Deep Eutectic Solvent: A Variety of Pb Species $PbSO_4$, PbO_2, and PbO Exhibits the Analogous Thermodynamic Behavior. *Electrochim. Acta* **2016**, *214*, 265−275.
(17) Bučko, M.; Culliton, D.; Betts, A. J.; Bajat, J. B. The Electrochemical Deposition of Zn−Mn Coating from Choline Chloride−Urea Deep Eutectic Solvent. *Trans. IMF* **2017**, *95*, 60−64.
(18) Francisco, M.; van den Bruinhorst, A.; Kroon, M. C. Low-Transition-Temperature Mixtures (LTTMs): A New Generation of Designer Solvents. *Angew. Chem., Int. Ed.* **2013**, *52*, 3074−3085.
(19) Dong, J.-Y.; Hsu, Y.-J.; Wong, D. S.-H.; Lu, S.-Y. Growth of ZnO Nanostructures with Controllable Morphology Using a Facile Green Antisolvent Method. *J. Phys. Chem. C* **2010**, *114*, 8867−8872.
(20) Gorke, J. T.; Srienc, F.; Kazlauskas, R. J. Hydrolase-Catalyzed Biotransformations in Deep Eutectic Solvents. *Chem. Commun.* **2008**, 1235−1237.
(21) Vanommeslaeghe, K.; Hatcher, E.; Acharya, C.; Kundu, S.; Zhong, S.; Shim, J.; Darian, E.; Guvench, O.; Lopes, P.; Vorobyov, I.; Mackerell, A. D. Charmm General Force Field: A Force Field for Drug-Like Molecules Compatible with the Charmm All-atom Additive Biological Force Fields. *J. Comput. Chem.* **2010**, *31*, 671−690.
(22) Kashyap, H. K.; Santos, C. S.; Annapureddy, H. V. R.; Murthy, N. S.; Margulis, C. J.; Castner, E. W., Jr. Temperature-Dependent Structure of Ionic Liquids: X-ray Scattering and Simulations. *Faraday Discuss.* **2012**, *154*, 133−143.
(23) Kashyap, H. K.; Santos, C. S.; Murthy, N. S.; Hettige, J. J.; Kerr, K.; Ramati, S.; Gwon, J. H.; Gohdo, M.; Lall-Ramnarine, S. I.; Wishart, J. F.; Margulis, C. J.; Castner, E. W. Structure of 1-Alkyl-1-methylpyrrolidinium Bis(trifluoromethylsulfonyl)amide Ionic Liquids with Linear, Branched, and Cyclic Alkyl Groups. *J. Phys. Chem. B* **2013**, *117*, 15328−15337.
(24) Annapureddy, H. V. R.; Kashyap, H. K.; De Biase, P. M.; Margulis, C. J. What is the Origin of the Prepeak in the X-ray Scattering of Imidazolium-Based Room-Temperature Ionic Liquids? *J. Phys. Chem. B* **2010**, *114*, 16838−16846.
(25) Kashyap, H. K.; Margulis, C. J. (Keynote) Theoretical Deconstruction of the X-ray Structure Function Exposes Polarity Alternations in Room Temperature Ionic Liquids. *ECS Trans.* **2013**, *50*, 301−307.
(26) Sharma, S.; Gupta, A.; Dhabal, D.; Kashyap, H. K. Pressure-Dependent Morphology of Trihexyl(tetradecyl)phosphonium Ionic Liquids: A Molecular Dynamics Study. *J. Chem. Phys.* **2016**, *145*, 134506.
(27) Sharma, S.; Gupta, A.; Kashyap, H. K. How the Structure of Pyrrolidinium Ionic Liquids Is Susceptible to High Pressure. *J. Phys. Chem. B* **2016**, *120*, 3206−3214.
(28) Agrawal, S.; Kashyap, H. K. Structures of Binary Mixtures of Ionic Liquid 1-Butyl-3-methylimidazolium Bis-(trifluoromethylsulfonyl)imide with Primary Alcohols: The Role of Hydrogen-Bonding. *J. Mol. Liq.* **2018**, *261*, 337−349.
(29) Gupta, A.; Sharma, S.; Kashyap, H. K. Composition Dependent Structural Organization in Trihexyl(tetradecyl)phosphonium Chloride Ionic Liquid-Methanol Mixtures. *J. Chem. Phys.* **2015**, *142*, 134503.
(30) Abbott, A. P.; Capper, G.; Davies, D. L.; Rasheed, R. K.; Tambyrajah, V. Novel solvent properties of choline chloride/urea mixtures. *Chem. Commun.* **2003**, 70−71.
(31) Phadtare, S. B.; Shankarling, G. S. Halogenation Reactions in Biodegradable Solvent: Efficient Bromination of Substituted 1-Aminoanthra-9,10-quinone in Deep Eutectic Solvent (Choline Chloride: Urea). *Green Chem.* **2010**, *12*, 458−462.
(32) Lindberg, D.; de la Fuente Revenga, M.; Widersten, M. Deep Eutectic Solvents (DESs) Are Viable Cosolvents for Enzyme-Catalyzed Epoxide Hydrolysis. *J. Biotechnol.* **2010**, *147*, 169−171.
(33) Li, X.; Hou, M.; Han, B.; Wang, X.; Zou, L. Solubility of CO_2 in a Choline Chloride + Urea Eutectic Mixture. *J. Chem. Eng. Data* **2008**, *53*, 548−550.
(34) Su, W. C.; Wong, D. S. H.; Li, M. H. Effect of Water on Solubility of Carbon Dioxide in (Aminomethanamide + 2-Hydroxy-n,n,n-trimethylethanaminium Chloride). *J. Chem. Eng. Data* **2009**, *54*, 1951−1955.
(35) Hayyan, M.; Mjalli, F. S.; Hashim, M. A.; AlNashef, I. M. A Novel Technique for Separating Glycerine from Palm Oil-based Biodiesel Using Ionic Liquids. *Fuel Process. Technol.* **2010**, *91*, 116−120.
(36) Abbott, A. P.; Capper, G.; Davies, D. L.; McKenzie, K. J.; Obi, S. U. Solubility of Metal Oxides in Deep Eutectic Solvents Based on Choline Chloride. *J. Chem. Eng. Data* **2006**, *51*, 1280−1282.
(37) Theophanides, T.; Harvey, P. D. Structural and Spectroscopic Properties of Metal-Urea Complexes. *Coord. Chem. Rev.* **1987**, *76*, 237−264.
(38) Thanu, D. P. R.; Raghavan, S.; Keswani, M. Use of Urea-Choline Chloride Eutectic Solvent for Back End of Line Cleaning Applications. *Electrochem. Solid-State Lett.* **2011**, *14*, H358−H361.
(39) Morrison, H. G.; Sun, C. C.; Neervannan, S. Characterization of Thermal Behavior of Deep Eutectic Solvents and Their Potential As Drug Solubilization Vehicles. *Int. J. Pharm.* **2009**, *378*, 136−139.
(40) Kaur, S.; Sharma, S.; Kashyap, H. K. Bulk and Interfacial Structures of Reline Deep Eutectic Solvent: A Molecular Dynamics Study. *J. Chem. Phys.* **2017**, *147*, 194507.
(41) Sun, H.; Li, Y.; Wu, X.; Li, G. Theoretical Study on the Structures and Properties of Mixtures of Urea and Choline Chloride. *J. Mol. Model.* **2013**, *19*, 2433−2441.
(42) Shah, D.; Mjalli, F. S. Effect of Water on the Thermo-Physical Properties of Reline: An Experimental and Molecular Simulation Based Approach. *Phys. Chem. Chem. Phys.* **2014**, *16*, 23900−23907.
(43) D'Agostino, C.; Gladden, L. F.; Mantle, M. D.; Abbott, A. P.; Ahmed, E. I.; Al-Murshedi, A. Y. M.; Harris, R. C. Molecular and Ionic Diffusion in Aqueous—Deep Eutectic Solvent Mixtures: Probing Inter-molecular Interactions Using PFG NMR. *Phys. Chem. Chem. Phys.* **2015**, *17*, 15297−15304.
(44) Hammond, O. S.; Bowron, D. T.; Edler, K. J. The Effect of Water upon Deep Eutectic Solvent Nanostructure: An Unusual Transition from Ionic Mixture to Aqueous Solution. *Angew. Chem., Int. Ed.* **2017**, *56*, 9782−9785.
(45) Posada, E.; López-Salas, N.; Jiménez Riobóo, R. J.; Ferrer, M. L.; Gutiérrez, M. C.; del Monte, F. Reline Aqueous Solutions Behaving As Liquid Mixtures of H-bonded Co-solvents: Microphase Segregation and Formation of Co-continuous Structures As Indicated

DOI: 10.1021/acsomega.8b02447
ACS Omega 2018, 3, 15246−15255

by Brillouin and ^{1}H NMR Spectroscopies. *Phys. Chem. Chem. Phys.* **2017**, *19*, 17103−17110.
(46) Fetisov, E. O.; Harwood, D. B.; Kuo, I.-F. W.; Warrag, S. E. E.; Kroon, M. C.; Peters, C. J.; Siepmann, J. I. First-Principles Molecular Dynamics Study of a Deep Eutectic Solvent: Choline Chloride/Urea and Its Mixture with Water. *J. Phys. Chem. B* **2018**, *122*, 1245−1254.
(47) Pandey, A.; Pandey, S. Solvatochromic Probe Behavior within Choline Chloride-based Deep Eutectic Solvents: Effect of Temperature and Water. *J. Phys. Chem. B* **2014**, *118*, 14652−14661.
(48) Hess, B.; Kutzner, C.; van der Spoel, D.; Lindahl, E. Gromacs 4: Algorithms for Highly Efficient, Load-Balanced, and Scalable Molecular Simulation. *J. Chem. Theory Comput.* **2008**, *4*, 435−447.
(49) Van Der Spoel, D.; Lindahl, E.; Hess, B.; Groenhof, G.; Mark, A. E.; Berendsen, H. J. C. Gromacs: Fast, Flexible, and Free. *J. Comput. Chem.* **2005**, *26*, 1701−1718.
(50) MacKerell, A. D.; Wiorkiewicz-Kuczera, J.; Karplus, M. An All-atom Empirical Energy Function for the Simulation of Nucleic Acids. *J. Am. Chem. Soc.* **1995**, *117*, 11946−11975.
(51) Yadav, A.; Pandey, S. Densities and Viscosities of (Choline Chloride + Urea) Deep Eutectic Solvent and Its Aqueous Mixtures in the Temperature Range 293.15 K to 363.15 K. *J. Chem. Eng. Data* **2014**, *59*, 2221−2229.
(52) Berendsen, H. J. C.; Grigera, J. R.; Straatsma, T. P. The Missing Term in Effective Pair Potentials. *J. Phys. Chem.* **1987**, *91*, 6269−6271.
(53) Martínez, L.; Andrade, R.; Birgin, E. G.; Martínez, J. M. Packmol: A Package for Building Initial Configurations for Molecular Dynamics Simulations. *J. Comput. Chem.* **2009**, *30*, 2157−2164.
(54) Darden, T.; York, D.; Pedersen, L. Particle mesh Ewald: An N·log(N) method for Ewald sums in large systems. *J. Chem. Phys.* **1993**, *98*, 10089−10092.
(55) Essmann, U.; Perera, L.; Berkowitz, M. L.; Darden, T.; Lee, H.; Pedersen, L. G. A Smooth Particle Mesh Ewald Method. *J. Chem. Phys.* **1995**, *103*, 8577−8593.
(56) Nosé, S. A Unified Formulation of the Constant Temperature Molecular Dynamics Methods. *J. Chem. Phys.* **1984**, *81*, 511−519.
(57) Nosé, S. A Molecular Dynamics Method for Simulations in the Canonical Ensemble. *Mol. Phys.* **1984**, *52*, 255−268.
(58) Hoover, W. G. Canonical Dynamics: Equilibrium Phase-Space Distributions. *Phys. Rev. A: At., Mol., Opt. Phys.* **1985**, *31*, 1695−1697.
(59) Parrinello, M.; Rahman, A. Polymorphic transitions in single crystals: A new molecular dynamics method. *J. Appl. Phys.* **1981**, *52*, 7182−7190.
(60) *International Tables for Crystallography*; Prince, E., Ed.; International Union of Crystallography, 2006; Vol. *C*.
(61) Brehm, M.; Kirchner, B. TRAVIS—A Free Analyzer and Visualizer for Monte Carlo and Molecular Dynamics Trajectories. *J. Chem. Inf. Model.* **2011**, *51*, 2007−2023.
(62) Humphrey, W.; Dalke, A.; Schulten, K. VMD: Visual Molecular Dynamics. *J. Mol. Graphics* **1996**, *14*, 33−38.
(63) Gao, Q.; Zhu, Y.; Ji, X.; Zhu, W.; Lu, L.; Lu, X. Effect of water concentration on the microstructures of choline chloride/urea (1:2) /water mixture. *Fluid Phase Equilib.* **2018**, *470*, 134−139.
(64) Hammond, O. S.; Li, H.; Westermann, C.; Al-Murshedi, A. Y. M.; Endres, F.; Abbott, A. P.; Warr, G. G.; Edler, K. J.; Atkin, R. Nanostructure of the Deep Eutectic Solvent/Platinum Electrode Interface As a Function of Potential and Water Content. *Nanoscale Horiz.* **2018**, DOI: 10.1039/C8NH00272J.

DOI: 10.1021/acsomega.8b02447
ACS Omega 2018, 3, 15246−15255